Zygmunt Mikno

# Cross Wire Projection Welding of Aluminium Alloy Bars (FEM 2.5D Calculations)

**Abstract:** The research described in the article involved the analysis of the cross wire projection welding of bars in relation to a conventional, i.e. pneumatic and a servomechanical electrode force system. The analysis was performed using Sorpas (2.5D model) software. Numerical calculations involved bars made of aluminium alloy 5182 (ϕ 4.0 mm) as well as to various values of electrode force (pneumatic system) and electrode travel (servomechanical system). The analysis involved the projection height reduction before and during the flow of current, the waveforms of static slope resistance, momentary power, weld diameter and the volume of molten material. The research aimed to optimise the process in relation to electrode force and/or electrode travel control in order to obtain such control of welding power space distribution so that energy could be concentrated in the central zone of the weld, where the use of the pneumatic system resulted in the obtainment of incomplete fusion instead of penetration. The article provides general recommendations concerned with the optimisation of a welding process involving the use of a servomechanical electrode force system.

**Keywords:** cross wire projection welding, numerical calculations, aluminium alloy 5182, servomechanical electrode force system

**DOI:** *10.17729/ebis.2017.4/1*

## Introduction

Because of characteristic, naturally formed or intentionally made projections, the welding of bolts nuts or sheets/plates with embossed projections as well as the short-circuit butt welding of bars or the cross wire welding of bars is treated as projection welding. Projections trigger an appropriate flow of current and ensure the proper course of the welding process. The article is concerned with the cross wire projection welding of bars.

In addition to the value of welding current and the time of welding current flow, electrode force is a parameter related to the resistance welding process, particularly important in projection welding. When applying the process of cross wire projection welding (particularly in relation to aluminium alloys), particularly

dr inż. Zygmunt Mikno (PhD (DSc) Eng.) – Instytut Spawalnictwa, Department of Resistance and Friction Welding and Environmental Engineering

when combined with the use of the conventional, i.e. pneumatic electrode force system, it is very difficult to obtain the complete (molten) weld nugget.

The pneumatic electrode force system is characterised by significant inertia entailing various problems particularly unfavourable when fast changes in electrode force are needed. For this reason, the value of electrode pressure during welding is usually constant. As a result, excessive electrode force results ultimately in the excessive deformation of welded elements (bars). In turn, insufficient electrode force may result in the formation of welded joint imperfections (high temperature in the electrode-welded material contact area or liquid metal expulsion). In addition, in terms of pneumatic force systems, the value of force results from pressure set in a pneumatic cylinder, where the travel of electrodes results from this force and the changing mechanical resistance of welded materials affected by the metallurgical process.

An alternative solution could involve the use of another method enabling the exertion of force on elements being welded [1-6]. The article presents the comparison of the conventional, i.e. pneumatic electrode force system with the new, i.e. servomechanical force system. Available scientific publications do not contain information about such a manner of electrode force and electrode travel control as that presented in this article [7-9]. Publications [10] and [11] contain certain results concerning the issue presented in the article and connected with the cross wire welding of bars.

This article constitutes part of extensive research on the welding process analysed in relation to the application of changeable electrode force during the flow of current or in relation to the control of electrode travel. The new welding process control method involves the use of a servomechanical system. The tests performed and described in this publication involve the SORPAS 2.5D computational model.

## Numerical Calculations

The numerical calculations were made using the SORPAS software programme (model 2.5D and 3D) [12] enabling the performance of combined thermal (electric and mechanical) analyses. The 2.5D software programme model used in the calculations features a module enabling the complex analysis of a new solution, i.e. the control of welding machine electrode force using a servomechanical system. The obtained calculation results were used to identify the direction of welding process optimisation in relation to cross wire welding and force exerted by the servomechanical system. The calculations also involved the use of the 3D model, characterised by better process representation and higher computational accuracy. However, because of the lack of essential functions in the 3D model including the detection of expulsion or the course of electrode force as regards the control of electrode movement, the process optimisation was clarified using the 2.5D model and the results obtained using the 3D model were treated in the analysis as supplementary.

The cross wire projection welded joint is characterised by a very thin layer of molten (welded) material. In the above-named process, the weld is frequently formed in the solid

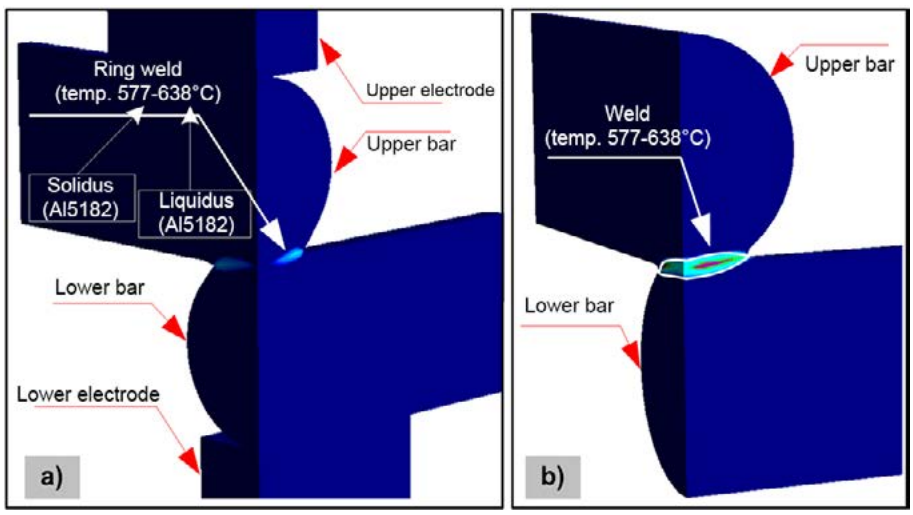


Fig. 1. Temperature distribution in the welding area (3D model)

state at a temperature below the melting point. The foregoing results from the specific course of the process, i.e. the melting of the material and the pushing the plasticised material outside the weld in the direction resulting from the electrode force. In such situations the weld takes a shape as presented in Figure 1a (ring weld, the lack of fusion in the central part).

The calculations involved bars made of aluminium alloy 5182 having a solidus temperature of 577°C and a liquidus temperature of 638°C [12]. The chemical composition of bars grade Al 5182 is presented in Table 1.

Table 1. Chemical composition of welded materials, i.e. bars grade Al 5182

| Al (max.) | Mn (max.) | Mg (max.) |
|---|---|---|
| 95.2 | 0.35 | 4.5 |

The results of numerical calculations indicated the formation of the ring weld, which impeded the performance of comparative analysis in relation to various welding parameters. For the purpose of better demonstration and detailed process analysis, in the FEM calculations the weld area was marked using an isothermal line representing a temperature of 530°C (Fig. 1b), the temperature below the melting point of the aluminium alloy subjected to the tests. It was assumed, following the statement by the author of publication [13], that the above-named temperature enabled the obtainment of a proper welded joint, further referred to as the weld and including the material above a temperature of 530°C.

## Computational Model

The FEM computational model (2.5D) related to the cross wire projection resistant welding of bars is presented in Figure 2. The model included the following assumptions: copper electrodes (A2/2), welded material in the form of aluminium bars AA5182 (designation in accordance with the SORPAS software database [12]) having a diameter of 4 mm and a 2.5D numerical model (1600 elements). The analysis included the pneumatic and servomechanical electrode force systems. The criteria adopted for calculations were the following:

1. maximum temperature at the point between the electrode and the welded bar: 500°C (mesh node no. 494 Fig. 2),
2. depth of bar penetration: max. 20% ($\Delta l$=1.6 mm),
3. lack of expulsion,
4. lack of deformation (bending) of bars,
5. maximum time of primary current flow: 60 ms.

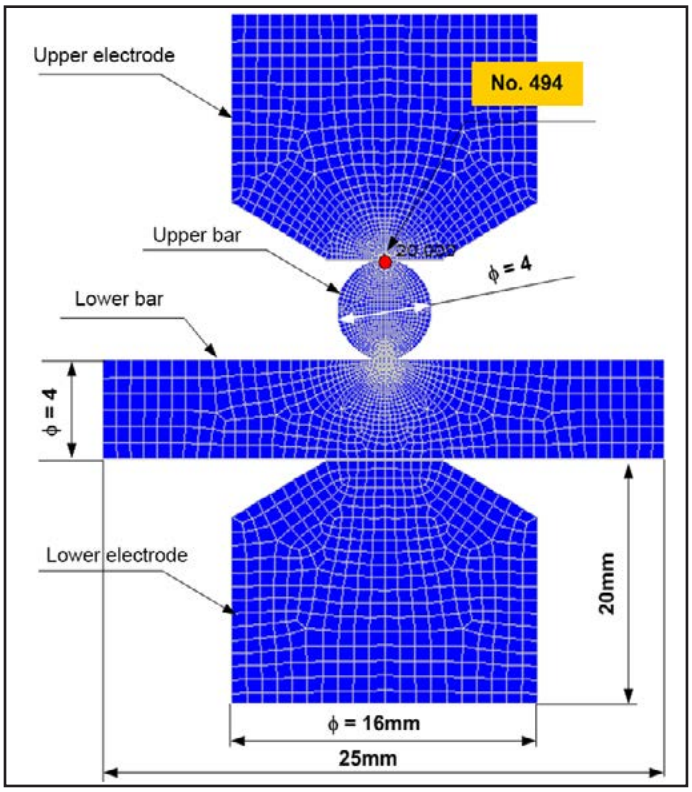


Fig. 2. FEM computational model related to the (cross wire) welding of aluminium bars (5182)

## Process Parameters

Numerical calculations related to the pneumatic force system were performed within a wide range of welding current values, i.e. 8-12 kA (every 2 kA), force 1.5 – 0.5 kN (every 0.5 kN) and the primary welding time amounting 60 ms and, additionally, "up-slope" (current increase time) amounting to 3 ms, for each combination of parameters [14], [15]. The remaining welding technology parameters included an initial force time of 20 ms and a final force time of 100 ms. The numerical calculations took

into consideration a DC inverter welding machine (1 kHz). The process optimisation was performed in relation to the servomechanical force system for the lowest analysed value of current in relation to the pneumatic system, i.e. 8 kA and, additionally, in relation to a lower value of 6 kA. The numerical calculations were continued until the occurrence or the exceeding of one of the assumed criteria.

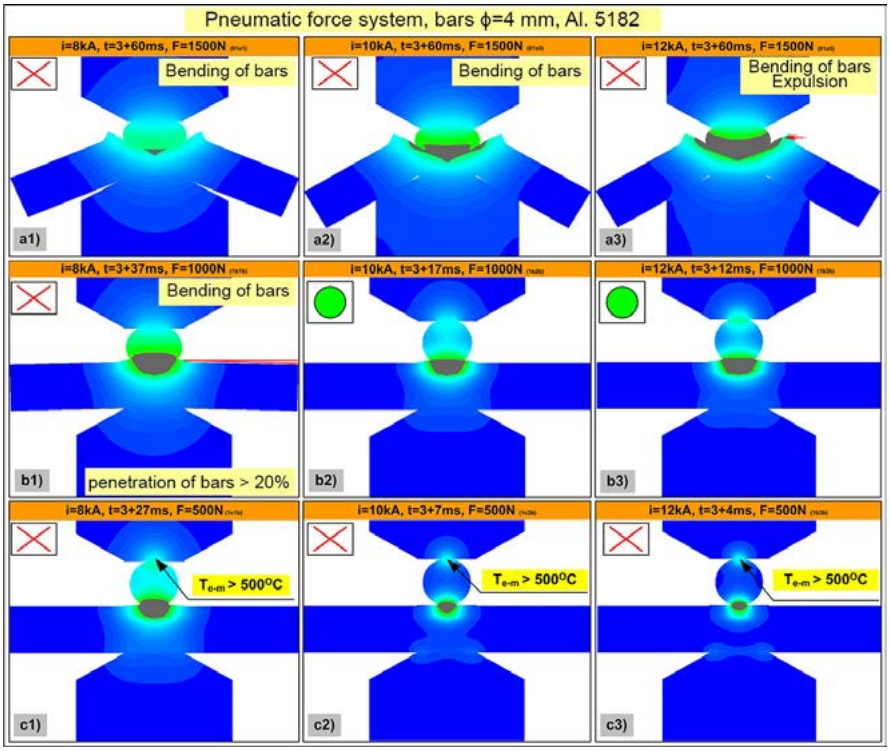


Fig. 3. Temperature distribution in the welding area, in relation to aluminium bars (5182) and the pneumatic force system, at the end of the welding process

## Results of Numerical Calculations

The results of the numerical calculations (in relation to aluminium bars 5182) are presented in Figures 3-5 and in Table 2. Figure 3 presents the distribution of temperature in the welding area, in relation to the pneumatic force system, at the end of the welding process (entire model) as well as

Table 2. Welding parameters, characteristic process-related quantities- FEM calculations (model 2.5D)

| No. | File name FEM calculations | Current kA | Time (slope+ primary time) ms | Force kN | Penetration $\Delta l$ mm | Weld diameter $mm^3$ | Weld volume kJ | Energy °C | $T_{e\text{-}m}$ no. 494 $T_{max}$ = 500°C | Remarks |
|---|---|---|---|---|---|---|---|---|---|---|
| | 1 | 2 | 3 | 4 | 5 | 6 | 7 | 8 | 9 | 10 |
| Pneumatic electrode force system | | | | | | | | | | |
| 1 | 01a1 | 8.0 | 3+60 | 1.5 | 3.0 | 1.4 | 2.1 | 234 | 351 | excessive penetration and bending of bars |
| 2 | 01a3 | 10.0 | 3+60 | | 4.1 | 4.8 | 23.0 | 322 | 448 | |
| 3 | 01a5 | 12.0 | 3+60 | | 3.6 | 5.6 | 48.9 | 328 | 460 | |
| 4 | 1b1b | 8.0 | 3+37 | 1.0 | 1.65 | 4.0 | 24.0 | 188 | 383 | |
| 5 | 1b2b | 10.0 | 3+17 | | 1.0 | 3.0 | 12.1 | 143 | 388 | OK, $\phi_{weld}$ > 3.0 mm |
| 6 | 1b3b | 12.0 | 3+12 | | 1.1 | 3.0 | 14.2 | 145 | 468 | |
| 7 | 1c1b | 8.0 | 3+27 | 0.5 | 0.4 | 2.8 | 13.2 | 167 | 500 | Temperature Te-m > 500°C, overly short weld diameter |
| 8 | 1c2b | 10.0 | 3+9 | | 0.1 | 1.9 | 6.0 | 94 | 526 | |
| 9 | 1c3b | 12.0 | 3+4 | | 0.1 | 1.8 | 6.1 | 66 | 528 | |
| 10 | 01b0 | 6.0 | 3+60 | 1.0 | 1.3 | 1.5 | 3.7 | 183 | 310 | nominal weld diameter < 3.0 mm |
| Servomechanical electrode force system | | | | | | | | | | |
| 11 | 11a1 | 8.0 | 3+32 | servo1 | 1.0 | 3.0 | 16.6 | 184 | 435 | OK, $\phi_{weld}$ = 3.0 mm |
| 12 | 21a2 | 6.0 | 3+57 | servo4 | 1.2 | 3.0 | 12.7 | 193 | 395 | |

in relation to various values of welding current and electrode force. Lines 1-10 of Table 2 present the results concerning the pneumatic force system, whereas lines 11 and 12 those related to the servomechanical force system. The red colour both in Fig 3 and Table 2 indicates exceeded and unacceptable parameters, whereas the green colour indicates results recognised as acceptable in relation to the servomechanical system and sufficiently favourable in relation to the pneumatic system.

## Analysis of Numerical Calculation Results

The analysis of the obtained numerical calculation results is presented below.

The ***electrode force of 1.5 kN*** proved excessively high and led to the excessive penetration of bars (Table 2, line 1, 2 and 3, column 5 - $\Delta l$= = 3.0 mm, 4.1 mm and 3.6 mm respectively) as well as to their excessive bending (deformation) (Fig. 3a1/a2/a3). The results led to the conclusion that the use of aluminium bars (5182) and of the pneumatic electrode force system should be accompanied by the application of lower electrode force.

The assumed weld diameter of 3 mm could be obtained using an ***electrode force of 1,0 kN*** only using higher welding current values, i.e. restricted within the range of 10.0 kA to 12.0kA (Table 2, line 5 and 6, column 6, Fig. 3b2/b3). The penetration of bars was restricted within the assumed range, below 20% of the total bar diameter thickness (Table 2, line 5 and 6 column 5). The bending of the bars was not observed (Fig. 3b2/b3). However, the value of current amounting to 8.0 kA was overly low to ensure the proper (intense) heating of the welding area. As a result, the weld diameter amounted to 4.0 mm, yet the penetration of the bars was excessive (Table 2, line 4, column 5, $\Delta l$ = =1.65 mm) and the bending of the bars could be observed (Fig. 3b1).

The use of ***electrode force amounting to 0.5 kN*** failed to satisfy the criterion concerning the obtainment of a required weld diameter (Table 2, line 7, 8 and 9, column 6, $\phi_{weld}$ = 2.8mm, 1.9 mm and 1.8 mm respectively and Fig. 3c1/c2/c3). When the force was lower, the critical parameter was the exceeding of temperature in the contact area between the electrode and the welded material above the assumed value of 500°C and the resultant phenomenon of expulsion. For this reason, it was necessary to reduce the time of welding, which, however, resulted in the obtainment of an overly short weld diameter.

## Process Optimisation

To better present the issue, the optimisation of the welding process was performed for the lower value of welding current (6.0 kA), which when combined with the use of the pneumatic electrode force system did not enable the obtainment of a welded joint. For comparison, calculations were performed in relation to the pneumatic force system exerting a force of 1.0 kN (regarded as the most favourable) and

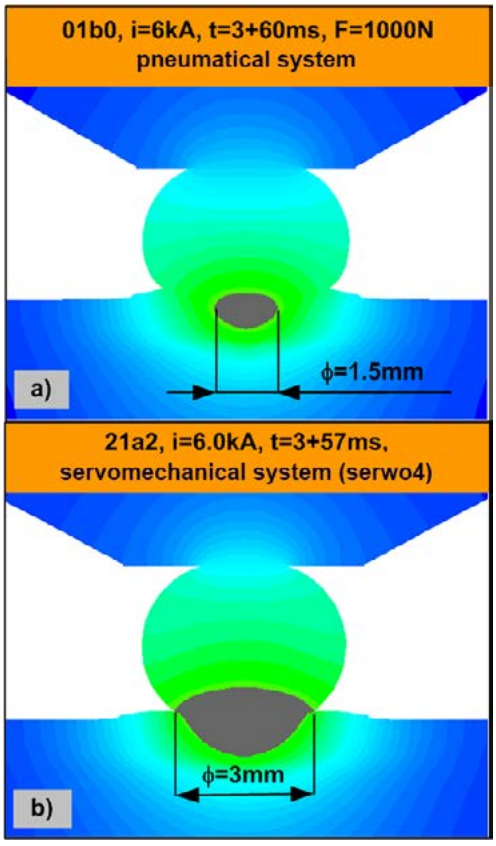


Fig. 4. Temperature distribution in the welding area in relation to welding current 6.0 kA: a) pneumatic system, b) servomechanical system

the entire process was subjected to optimisation applying the same lower value of welding current (6,0 kA) but using an appropriate force profile (course) related to the use of the servomechanical electrode force system. The results of the comparison in the form of temperature distribution images are presented in Figure 4. In turn, Table 2 contains results in the numerical form (line 11 and 12). The use of the servomechanical force system combined with the control of electrode travel during the flow of current enabled the obtainment of an assumed weld diameter of 3.0 mm.

The manner in which the process was optimised is presented in Figure 5. The initial point was the travel of electrodes (depth of bar penetration). The use of the pneumatic system led to the obtainment of an insufficient weld diameter amounting to 1.5 mm (Table 2, line 10, column 5). The overly low current only plasticised the material, leading to the obtainment of a significant contact area. The low welding current of 6.0 kA was characterised by overly low density. As a result, the material subjected to welding couldn't become molten but only heated and plasticised.

As regards the pneumatic system, the final value of bar penetration amounted to 1.3 mm (Fig. 5d, curve 1). In terms of the weld formation process, the above-named value as well as the curve characteristic were not favourable. The use of the servomechanical force system was dictated by the need for obtaining a lower final bar penetration value than that obtained using the pneumatic system, e.g. 0.8 mm (Fig. 5d, curve 3) and more favourable electrode movement trajectory. The obtained value of (momentary) power was higher within the entire range (Fig. 5c, curve 3) than that obtained using the pneumatic system (Fig. 5c, curve 1). Such a waveform of power enabled the obtainment of the nominal weld diameter

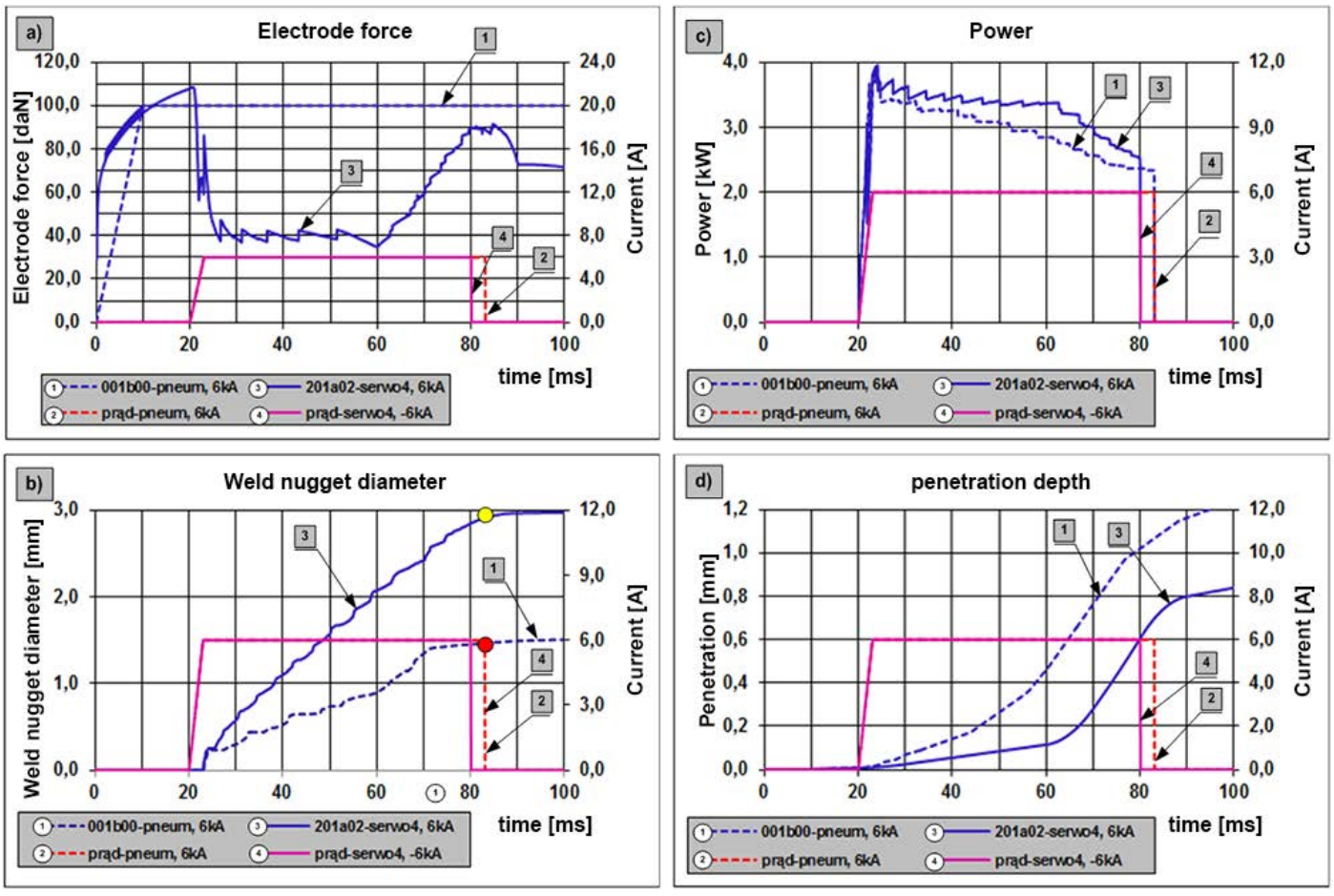


Fig. 5. FEM calculation results: a) electrode force, b) weld diameter, c) momentary power, d) depth of bar penetration. Curves: 1, 2) pneumatic electrode force ($I$=6.0 kA, $P$=1.0 kN), 3, 4) servomechanical electrode force ($I$=6.0 kA, servo4)

(3.0 mm) up to 63 ms (Fig. 5b, curve 3 and Table 2, line 12, column 6). The final result related to the servomechanical system control was the appropriate course of electrode force, affecting the value of resistance, particularly in the areas of contact (in the welded bar-welded bar configuration), providing the proper space distribution of welding power as well as proper temperature distribution in the welding area and, finally, leading to the melting of the material and the formation of a weld having a desired (greater) size.

The analysis concerning the welding current value amounting to 6.0 kA (proved overly low to obtain a proper joint using the pneumatic electrode force system) led to the conclusion that the use of the servomechanical system combined with the proper control (of electrode force and/or electrode travel) could improve the welding process and enable the obtainment of a greater weld diameter than that obtained using the pneumatic electrode force system.

## Summary

The assumed objective of the research was accomplished in full. It was demonstrated that the control of welding machine electrode travel provides significantly better results than that of electrode force. The control of electrode travel was performed using the servomechanical system and the results obtained were compared with those obtained using the pneumatic electrode force system. As regards the entire melting of the weld nugget, particularly in relation to the pneumatic electrode force system and materials characterised by high thermal and electric conductivity (e.g. aluminium alloys), the obtainment of cross wire welding parameters is very difficult or nearly impossible. These limitations result from the impossibility of quick force control during the process of welding. Importantly, the preset parameter is force (i.e. electrode force), whereas the resultant parameter is travel (i.e. electrode travel), not controlled in any manner whatsoever. The course of the welding process (the extension of the window of parameters) could be improved by using the servomechanical electrode force system. The operation mode involving the travel of electrodes enables the setting of more favourable electrode movement trajectory leading to the more favourable distribution of current density as well as to the more favourable space distribution of welding power, which, consequently, translates into the extension of the window (i.e. range) of welding parameters and the obtainment of a weld characterised by greater dimensions. The computational model used in the tests (Sorpas 2.5D) is not a perfect tool. However, because the 3D model lacks important programme functions in terms of process analysis, the 2.5D model is the only tool enabling the performance of complete analysis.

***The article contains results obtained within project TANGO1/267374/NCBR/2015 implemented in 2015-2017 and financed by the National Science Centre (NCN) and National Centre for Research and Development (NCBR).***

## References

[1] Zhang X., Chen G., Zhang Y., Lai H.: *Improvement of resistance spot weldability for dual-phase (DP600) steels using servo gun*. Journal of Materials Processing Technology, 2009, vol. 209, no. 5, pp. 2671-2675 http://dx.doi.org/10.1016/j.jmatprotec.2008.06.008

[2] Tang H., Hou W., Hu S.: *Forging force in resistance spot welding*. Proceedings of the Institution of Mechanical Engineers, Part B: Journal of Engineering Manufacture, 2002, vol. 216, no. 7. http://dx.doi.org/10.1243/09544050260174166

[3] Gould J.: *Joining Aluminum Sheet in the Automotive Industry – A 30 Year History*. Welding Journal (Welding Research), 2012, vol. 91, pp. 23-34.

[4] Agapiou J. S., Perry T. A.: *Resistance mash welding for joining of copper conductors for electric motors*. Journal of Manufacturing Processes, 2013, vol. 15, no. 4, pp. 549–557. http://dx.doi.org/10.1016/j.jmapro.2013.06.014

[5] Zhang X. Q., Chen G. L., Zhang Y. S.: *Online evaluation of electrode wear by servo gun in resistance spot welding*. International Journal of Advanced Manufacturing Technology, 2008, vol. 36, no. 7–8, pp 681–688. http://dx.doi.org/10.1007/s00170-006-0885-8

[6] Slavick S.A.: *Using Serwoguns for Automated Resistance Welding*. Welding Journal, 1999, vol. 78, no. 7.

[7] Mikno Z., Bartnik Z., Ambroziak A., Pietras A.: Patent P. 401723 *Method for Projection Resistance Welding of Steel Plates with Embossed Projections*. 2012.

[8] Mikno Z., Bartnik Z.: *Projection welding with pneumatic and servomechanical electrode pressure system in FEM calculation - comparison*. The 7th International Seminar on Advances in Resistance Welding, 12-14 September 2012, Busan, Korea.

[9] Mikno Z.: *Projection Welding with Pneumatic and Servomechanical Electrode Operating Force Systems*. Welding Journal (Welding Research), 2016, vol. 95, pp. 286-299.

[10] Mikno Z., Grzesik B., Stępień M.: Patent P. 412615 *Sposób zgrzewania rezystancyjnego garbowego w konfiguracji na krzyż zwłaszcza prętów aluminiowych*. 2015

[11] Mikno Z., Grzesik B., Stępień M.: *Cross-Wire Projection Welding of Aluminium Alloys in relation to Pneumatic and Servomechanical Electrode Force Systems*. 10th International Conference Trends in Welding Research, Tokyo, Japan, 11-14 October 2016.

[12] The database of the material and electrode parameters: model 2D version 11.2 and model 3D Version 4.0x64 of the Swantec Inc. SORPAS Software http://swantec.com/

[13] Xu W., Liu J., Luan G., Dong Ch.: *Temperature evolution, microstructure and mechanical properties of friction stir welded thick 2219-O aluminum alloy joints*. Material and Design, 2009, vol. 30, no. 6, pp. 1886-1893. http://dx.doi.org/10.1016/j.matdes.2008.09.021

[14] Papkala H.: *Zgrzewanie oporowe metali*. Wydawnictwo KaBe, Krosno, 2003.

[15] AWS Welding Handbook 9th edition, vol. 3, Welding Processes, part 2, chapter 2, Projection Welding

[16] Gould J. E.: *Projection Welding*. ASM International, ASM Handbook, vol. 6: Welding, Brazing, and Soldering. USA 1993, pp. 230-237